

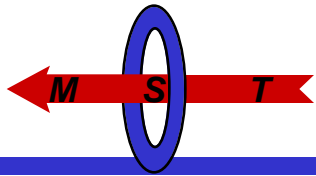
# Ion Heating and Energy Transport on MST

J. Reardon, T.M. Biewer, B.E. Chapman, D. Craig, G. Fiksel, S.C. Prager  
UW Madison

S. Terry  
UCLA

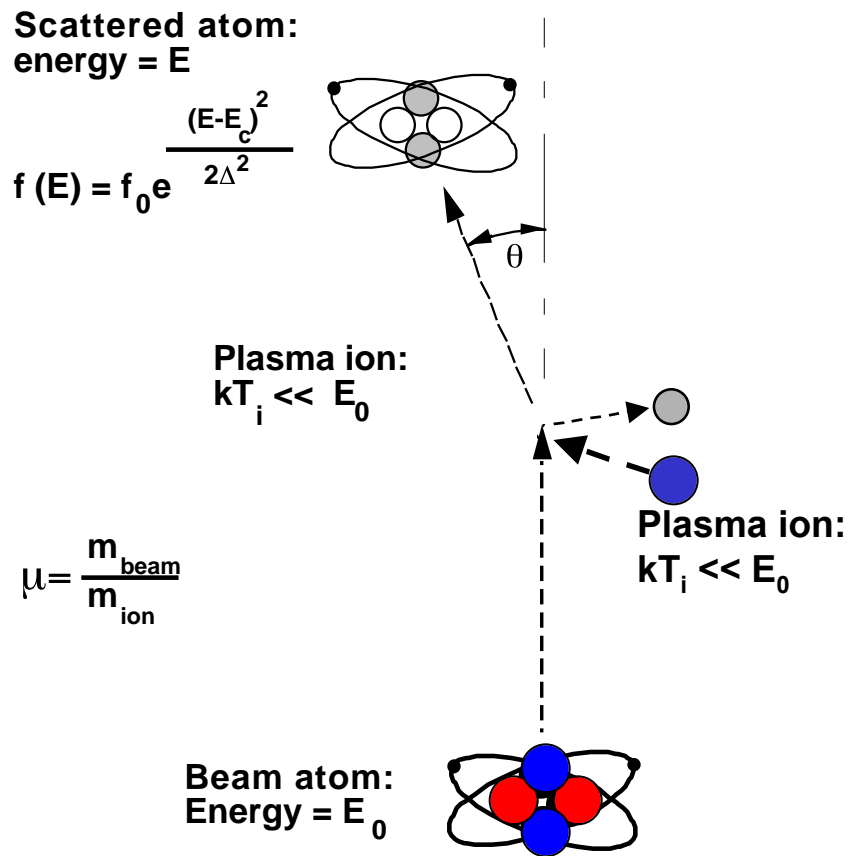
and the MST team

Ion temperatures are often measured to be higher in Reversed Field Pinch (RFP) plasmas than can be accounted for by energy transfer from ohmically-heated electrons. Recently the Madison Symmetric Torus (MST) has been reconfigured to allow the time, space, mass, and charge dependences of this excess heating to be sorted out. Shot-to-shot temperature profiles are acquired, for the bulk majority (Deuterium) ions by Rutherford Scattering (RS), and for impurities (Carbon) by the Charge Exchange Recombination Spectroscopy (CHERS). Anomalous ion heating occurs at Magnetic Reconnection Events (MREs). The relative importance of anomalous ion heating to the ion power balance is determined by comparison of measurements in standard and Pulsed Poloidal Current Drive (PPCD) discharges, which respectively do and do not experience MREs.



# Principle of Rutherford Scattering

$T_i$  found from width of energy spectrum of scattered atoms



Assume ideal beam  
(monoenergetic, zero  
angular dispersion)

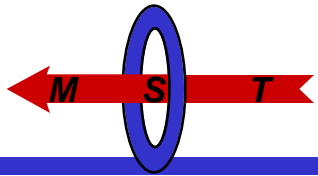
For scattering angle  $\theta$ ,  
energy spectrum of  
scattered atoms is  
approximately Gaussian:

Variance :

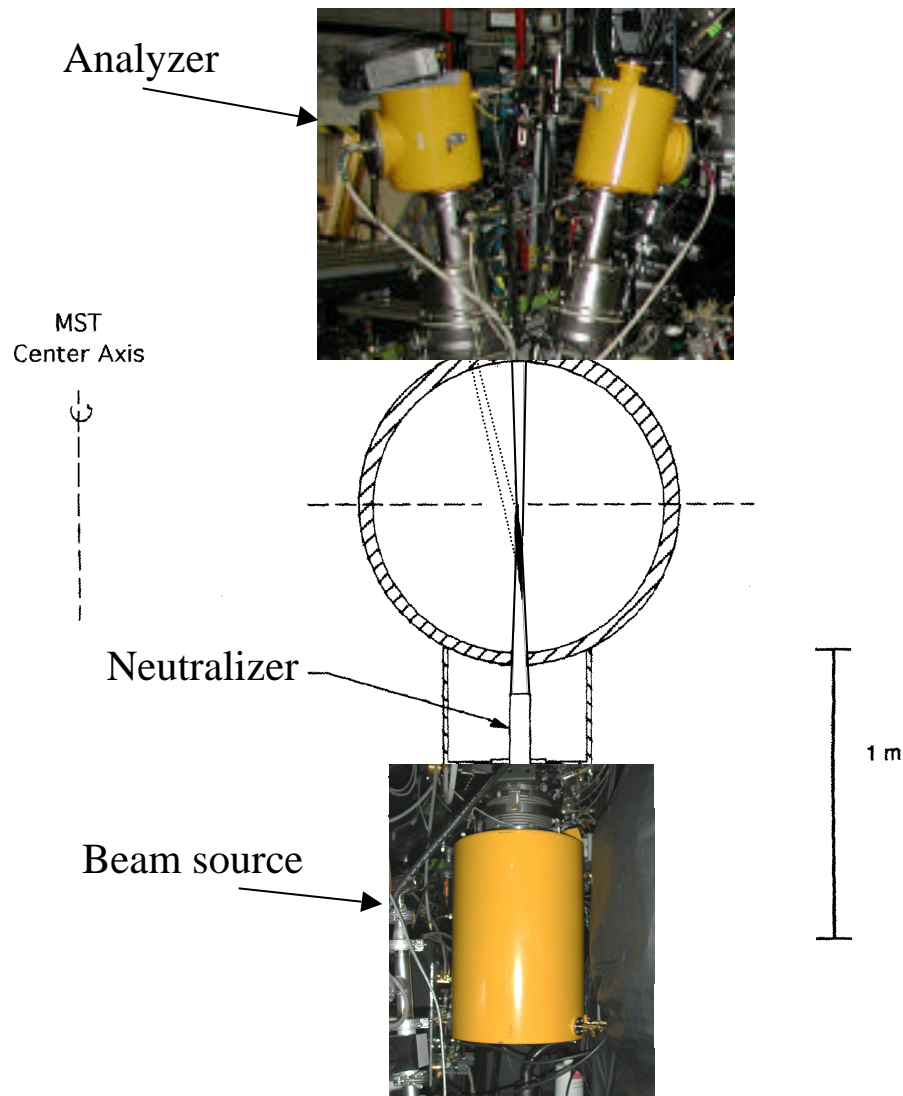
$$= \sqrt{2\mu E_0 T_i \theta^2}$$

Centroid  $E_c$  :

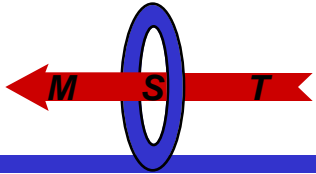
$$E_c = E_0 (1 - \mu \theta^2)$$



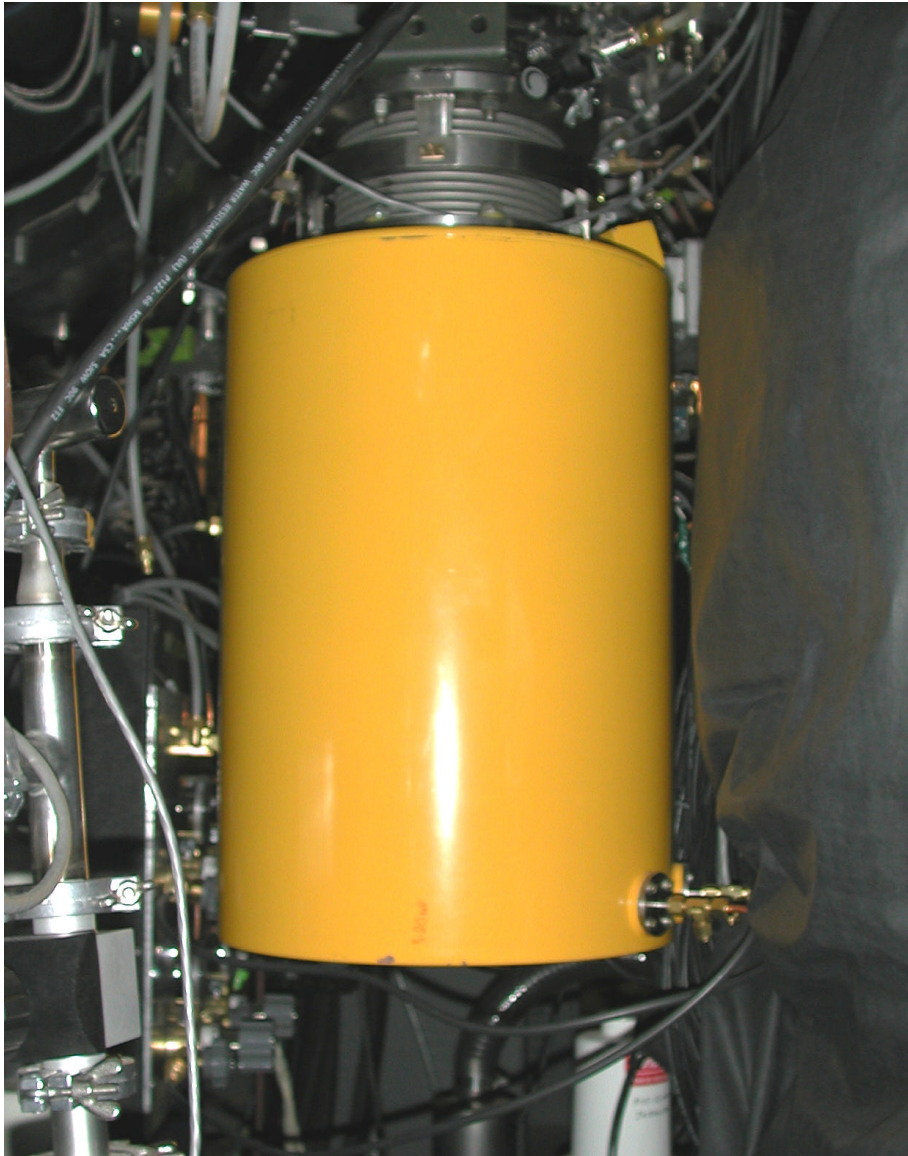
# Rutherford Scattering on MST



- Small-angle scattering of beam atoms by plasma ions
- Scattering volume  $\sim 30$  cm in minor radius
- Temperature profile acquired by tilting analyzer(s) between shots



# Diagnostic Neutral Beam Source



20 KeV Helium

4 A equivalent current

3 ms beam duration

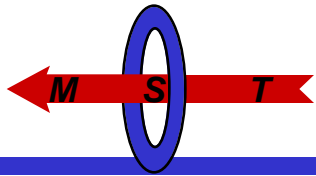
Energy spread  $E \sim 300 \text{ eV}$

Angular spread  $\sim 0.03$

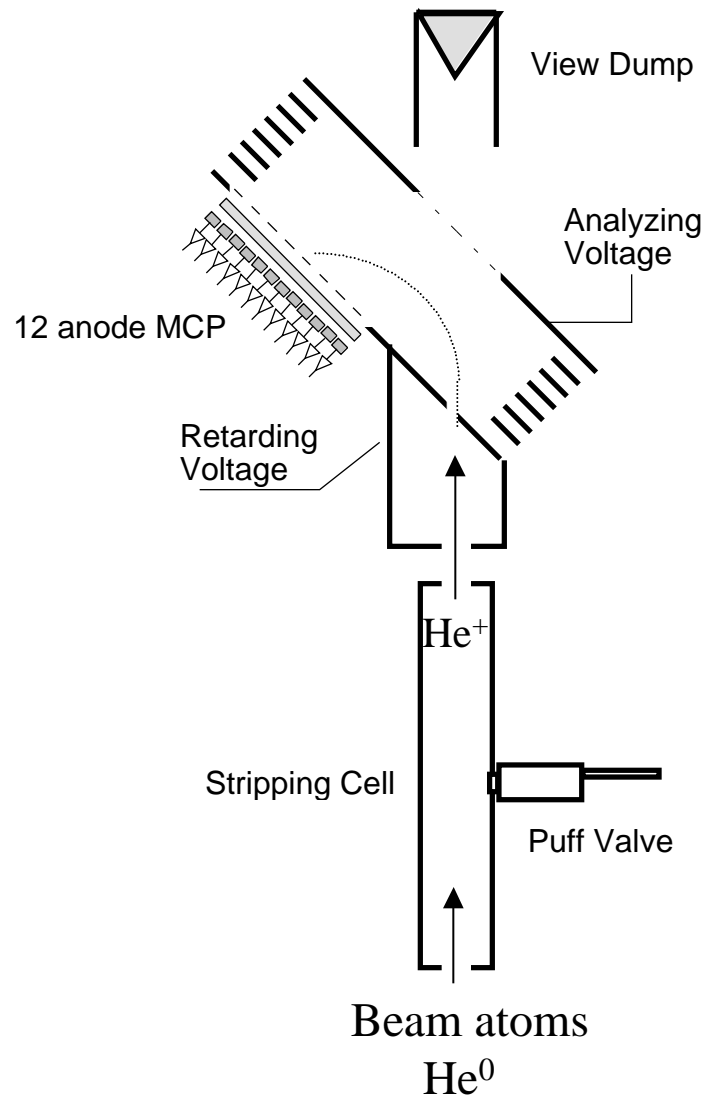
Built at Novosibirsk

Operated reliably on MST  
since December 1999

Weight: 40 kg



# Rutherford Analyzers



2 independent 12-channel electrostatic neutral particle analyzers

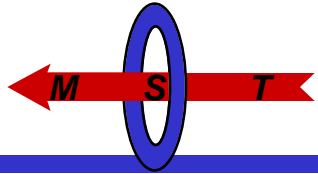
Each analyzer axis can be tilted (in toroidal and poloidal planes) or translated (in poloidal plane)

Transimpedance =  $10^9$  V/A

Built at Novosibirsk

Operated reliably on MST since December 1999

Weight: 60 kg



# Rutherford Scattering: History

---

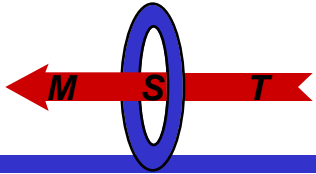
First described: E. Rutherford, *Philos. Mag.* **21**, 669 (1911).

First proposed as a  $T_i$  diagnostic:

Abramov et al, *Sov. Phys. Tech. Phys.* **16**, 1520 (1972).

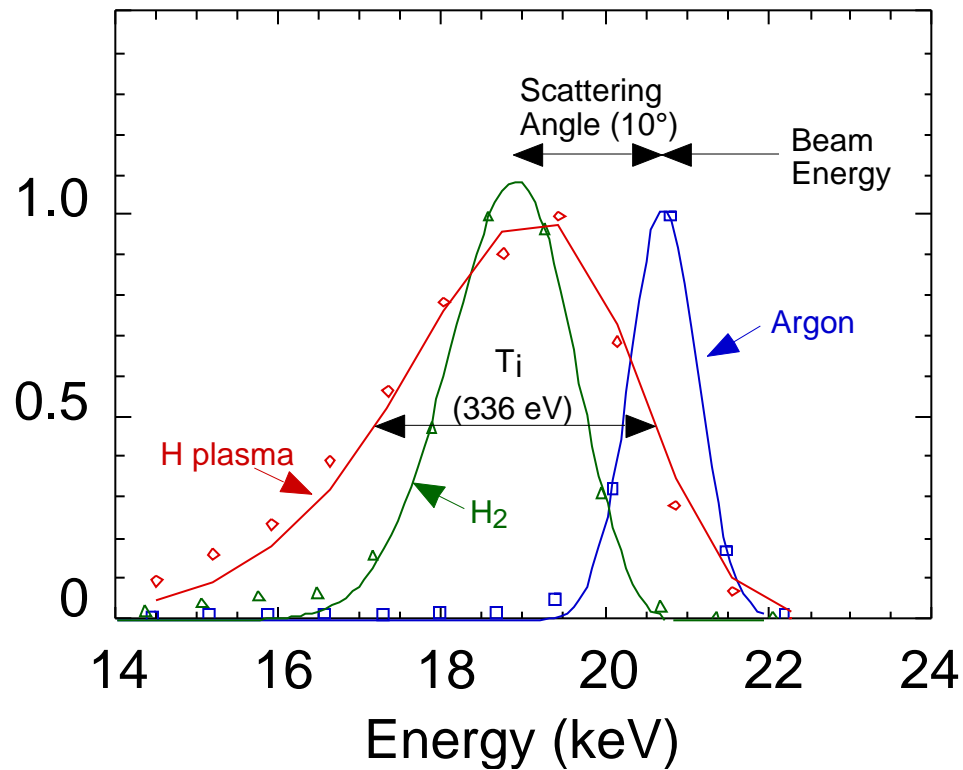
Uses by fusion community:

- T-4 Aleksandrov, et al., *JETP Letters* **29**, 1 (1979).
- JT-60 Tobita, et al., *Nucl. Fus.* **28**, 1719 (1988).
- TEXTOR van Blokland et al., *RSI* **63**, 3359 (1992).
- GDT (mirror) Anikeev et al., *Phys. Plas.* **4**, 347 (1997).
- MST (RFP) Reardon et al., *RSI* **72** 1 (2001)



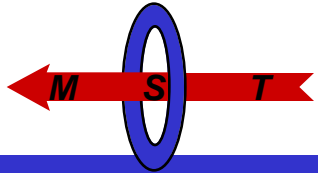
# Calibration

Normalized Scattering Spectra



- Scattering from Argon gas
  - Position - beam energy
- Scattering from Hydrogen gas
  - Position - scattering angle
  - Width - instrumental width
- Scattering from plasma
  - Width - ion temperature

For more information on RS calibration and analysis, see Reardon et al., RSI **72** 1 (2001)



# Temperature profile measurements

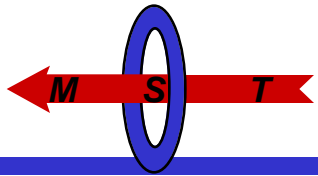
---

## Shot-to-shot temperature profiles now available of:

- Deuterium (bulk majority), using Rutherford scattering
  - ~ 25 discharges/location
  - ~ 5 locations/profile
  - First time local bulk majority temperature measurement on an RFP!
- Impurity ( $C^{VI}$ ), using charge-exchange recombination spectroscopy (CHERS)
  - ~ 5 discharges/chord
  - 11 chords currently available
  - First time local impurity measurement on MST!
- Electrons, using Thomson scattering
  - ~ 25 discharges/chord
  - 16 chords currently available

{Also shown will be line-averaged  $C^{+4}$  temperatures from the Impurity Dynamics Spectrometer (IDS), which doesn't return a profile but does have high time resolution ( $\sim 10 \mu s$ ).}

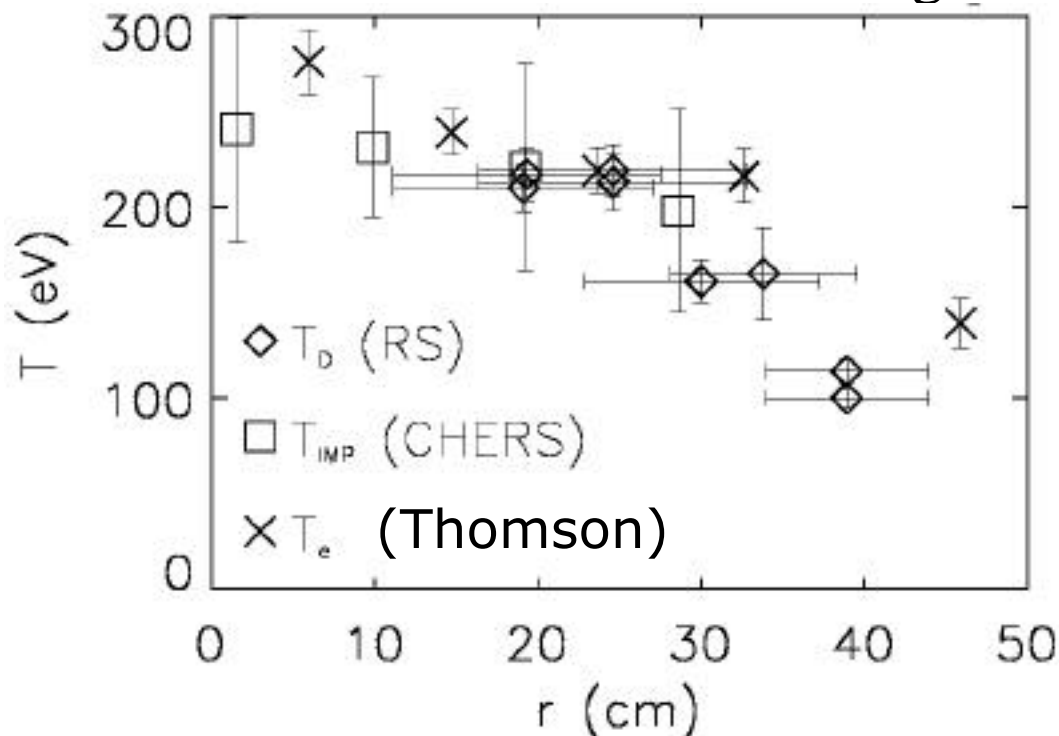




# $T_i \sim T_e$ in standard discharges

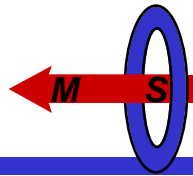
Ensemble average over all phases of MRE cycle.

380 kA Standard Discharges



Ensemble parameters:

- medium density  
( $8 \cdot 10^{12} \text{ cm}^{-3} < n_e < 1.1 \cdot 10^{13} \text{ cm}^{-3}$ )
- $f \sim -0.22$
- $I_p$  flat-top
- 25 shots/point (RS, Thomson)  
~10 shots/point (CHERS)

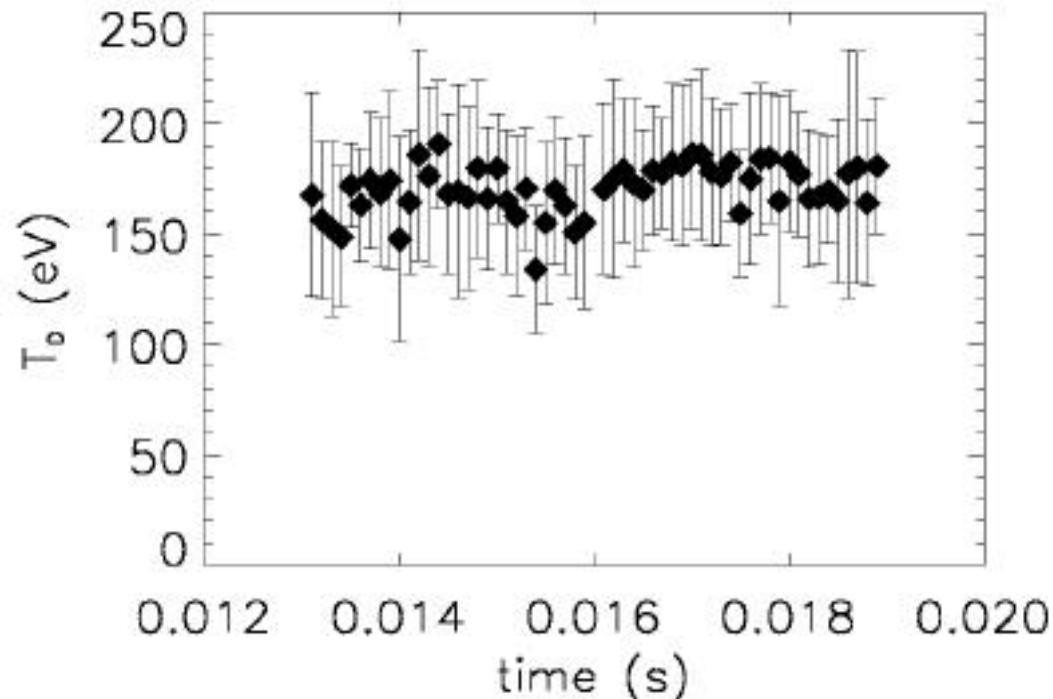


# $T_D$ does not evolve in standard discharges

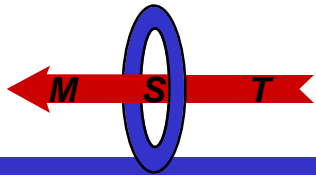
Ensemble average over all phases of the MRE cycle.

No secular evolution of  $T_D$  is seen.

380 kA Standard discharges



$T_D$  from Rutherford scattering at  $0.4 < r/a < 0.5$

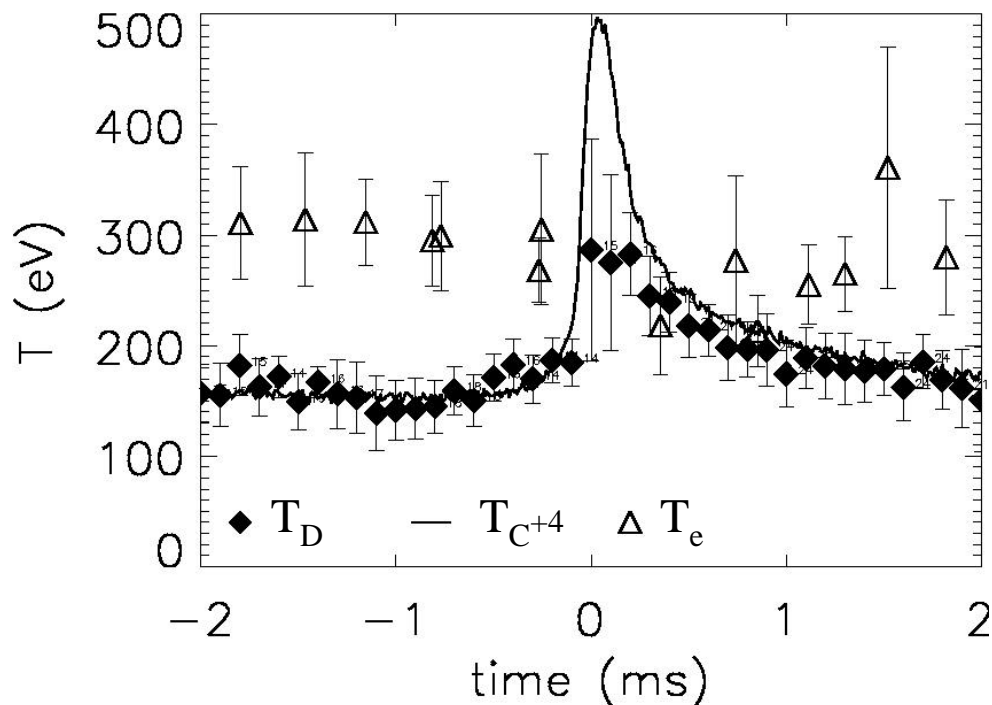


# Rapid increase in $T_{\text{Ion}}$ at MRE

$T_D$  from Rutherford scattering at  $0.4 < r/a < 0.5$  (35 crashes, on 2 June 2001)

$T_{C^{+4}}$  from Doppler emission (from  $C^{+4}$ )  $0.3 < r/a < 0.6$  (352 crashes, on 4 July 2001)

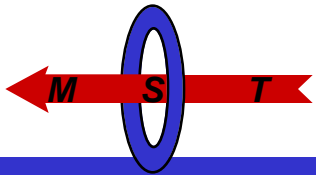
$T_e$  from Thomson scattering at  $0.4 < r/a < 0.5$  (~60 crashes, Nov 2000)



Ensemble parameters:

- medium density  
( $8 \cdot 10^{12} \text{ cm}^{-3} < n_e < 1.1 \cdot 10^{13} \text{ cm}^{-3}$ )
- $f \sim -0.22$
- $I_p = 380 \text{ kA}$

At the time of an MRE,  $T_{C^{+4}}$  increases by a factor of  $\sim 3$ ,  $T_D$  increases by  $\sim 50\%$ , while  $T_e$  remains nearly unchanged. Magnetic stored energy decreases by  $\sim 10 \text{ kJ}$  in  $\sim 50 \mu\text{s}$ .

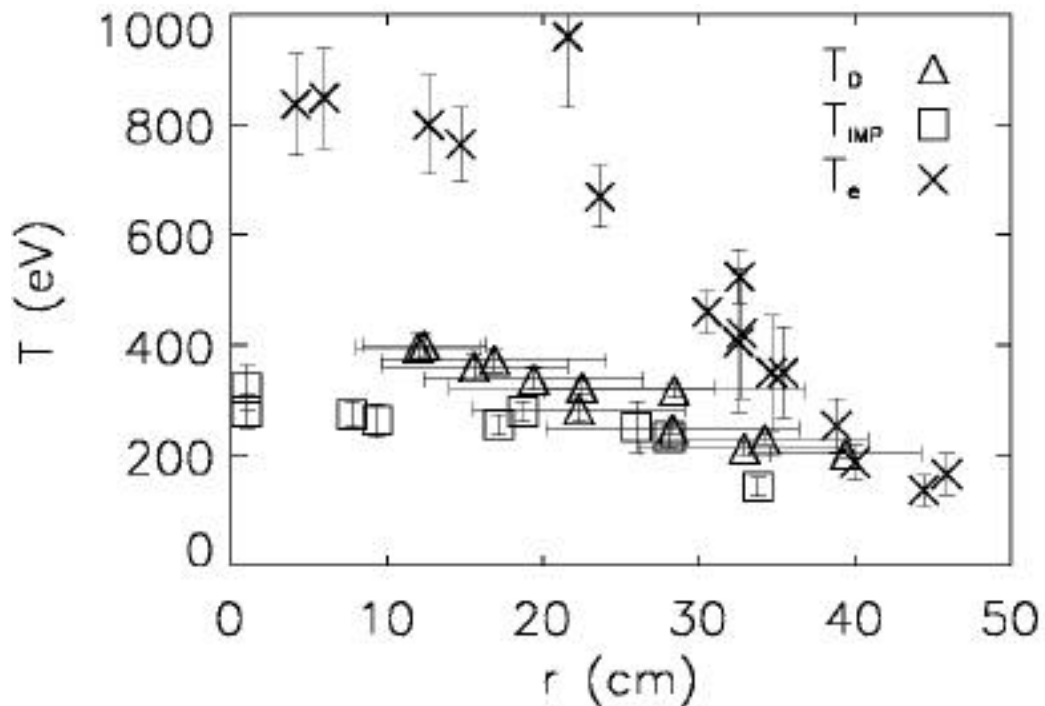


# PPCD heats electrons not ions

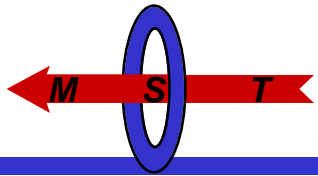
PPCD = Pulsed Poloidal Current Drive

PPCD broadens the current profile, suppresses fluctuations, and improves confinement (see Brett Chapman's talk tomorrow).

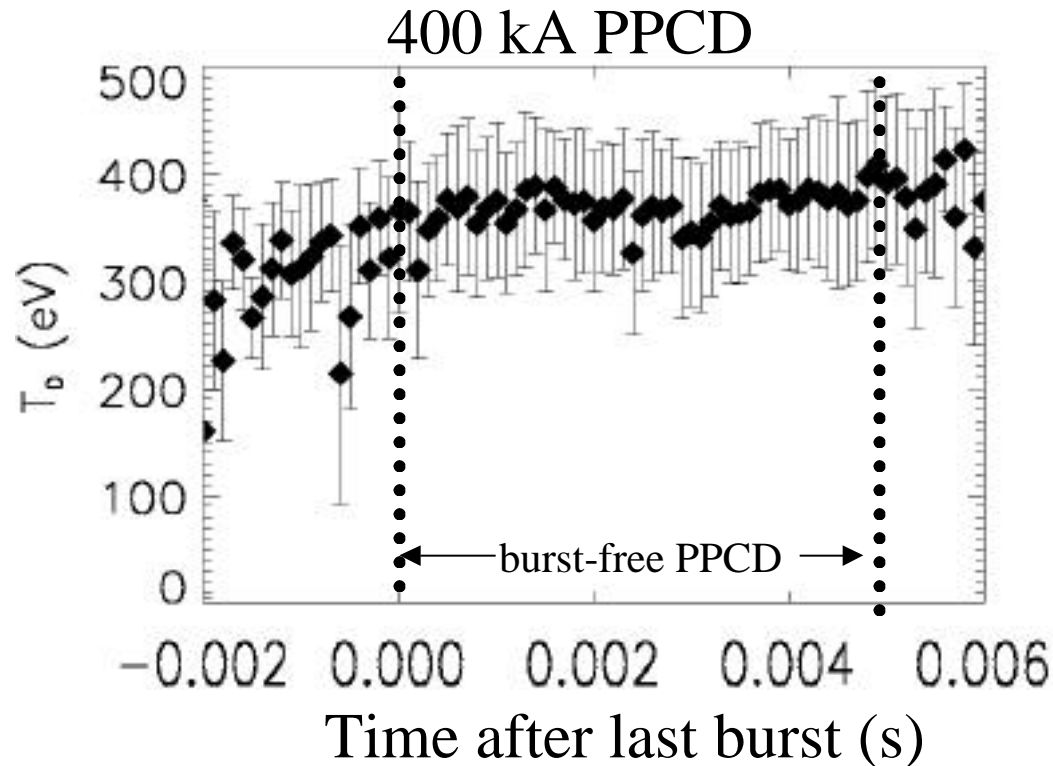
400 kA PPCD Discharges



- In PPCD discharges, as compared to standard discharges with the same  $I_p$ :
- $T_e(0)$  increases by a factor of  $>2$
  - $T_D \sim T_{imp}$  remains nearly unchanged
  - $n_e(0)$  increases by 30%
  - $Z_{eff}(0)$  increases, to 5



# $T_D$ is constant during burst-free PPCD



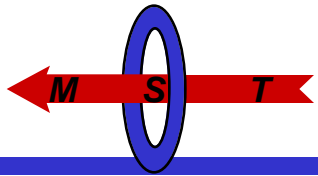
Ensemble parameters:

- ~100 shots
- burst free phase lasting longer than 5 ms

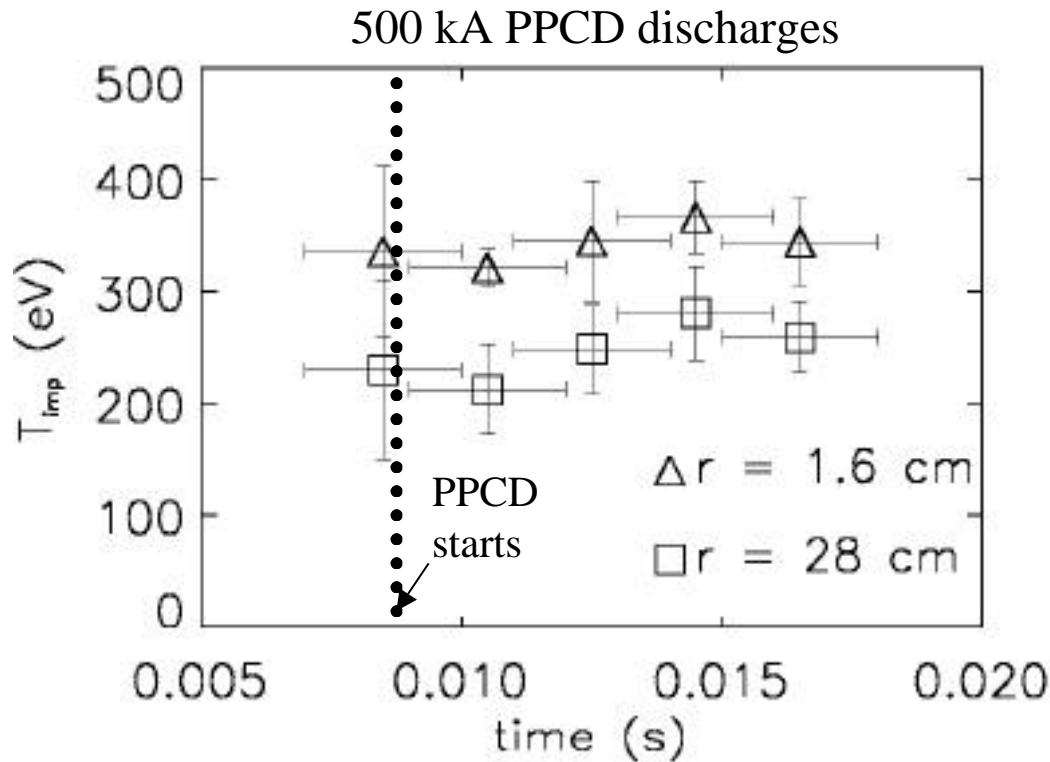
$T_C$  similar

$T_e$  increasing

$T_D$  from Rutherford scattering at  $r/a < 0.4$



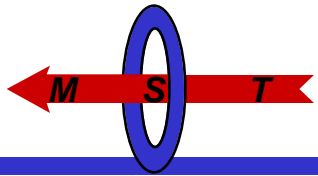
# $T_{\text{IMP}}$ is constant during PPCD



Ensemble parameters:

- ~5 shots/point
- average over bursts and burst-free times
- horizontal error bars reflect averaging time

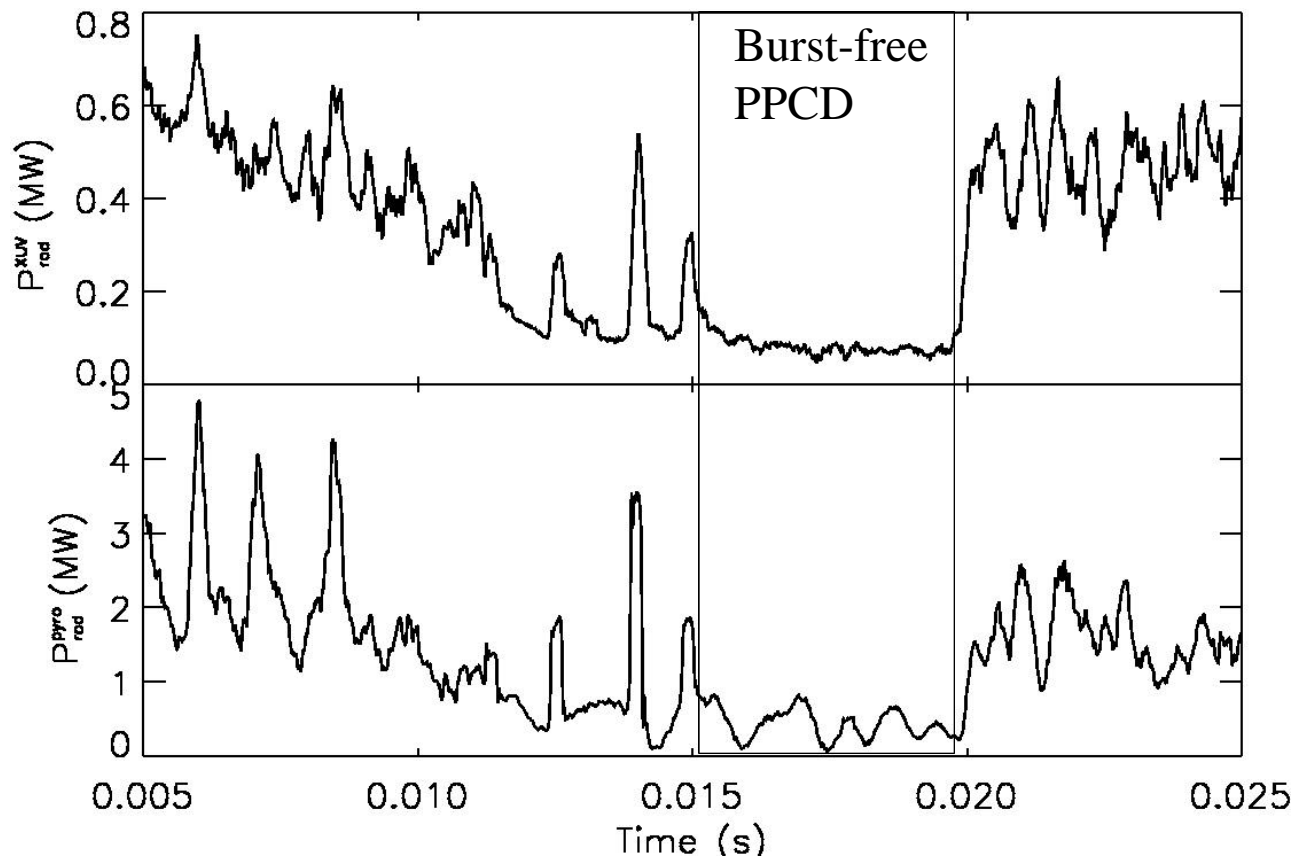
$T_{\text{C}+6}$  from CHERS

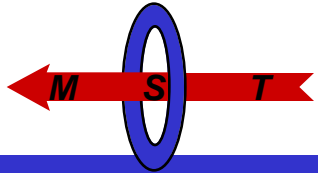


# Charge Exchange Loss in PPCD

XUV diode measures radiant heat flux.

Pyrobolometer measures both radiant and CX heat flux.





# Comparison of charge exchange losses

---

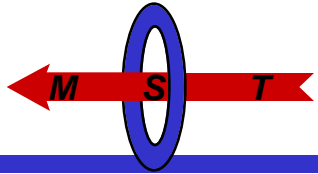
In burst-free periods lasting at least 5 ms,  
during 400 kA PPCD:

$$P_{CX} \sim 460 \text{ kW (ensembled over 350 shots)}$$

Compare to 380 kA standard discharges (between MREs):

$$P_{CX} \sim 1.1 \text{ MW (ensembled over 50 shots)}$$





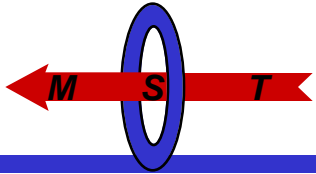
# Power balance strategy

---

Is classical ion heating sufficient to explain high ion temperatures?

- Use measured  $T_e$  and  $n_e$ , and estimated  $Z_{\text{eff}}$ , to calculate  $\tau_{eq}^{i,e}$ .  
(The largest source of error will be in the estimate of  $Z_{\text{eff}}$ .)
- Use measured  $T_e$ ,  $T_i$ , and  $n_e$  profiles, and estimated  $Z_{\text{eff}}$  profile, to estimate  $P_{e,i}$ , the total classical power flow into ions.
- Calculate the known channel of power flow from ions, namely charge-exchange loss  $P_{\text{CX}}$ , from pyrobolometer and XUV diode.

If  $P_{\text{CX}}$  is larger than  $P_{e,i}$ , then classical ion heating is not sufficient to explain high ion temperatures.



# Power balance for Ions

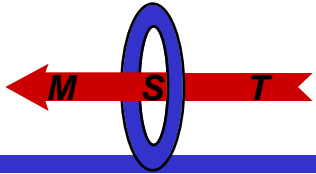
Power balance equation for ions:

$$\frac{3}{2} n_D \frac{\partial T_D}{\partial t} = \sum_{k=e,i} \frac{3}{2} n_D \frac{(T_k - T_D)}{\tau_{eq}^{j,k}} + P_{anom} - P_{CX} - P_{other}$$

where the energy equilibration time between species j,k is defined as:

$$\tau_{eq}^{j,k} = \frac{3\sqrt{2}\pi^{3/2}\epsilon_0^2 m_j m_k}{n_k Z_k^2 Z_j^2 e^4 \ln_{jk} \left( \frac{T_j}{m_j} + \frac{T_k}{m_k} \right)^{3/2}}$$

$$\begin{aligned} \text{using: } \ln_{jk} &= \frac{\lambda_d}{b_{90}} = \frac{12\pi\epsilon_0^{3/2} T_e^{1/2} (\sqrt{T_j m_k} + \sqrt{T_k m_j})^2}{Z_j Z_k n_e^{1/2} e^3 (m_j + m_k)} \\ &= 9 \frac{4\pi}{3} n_e \lambda_d^3 \quad \text{if either } j, k = e \end{aligned}$$



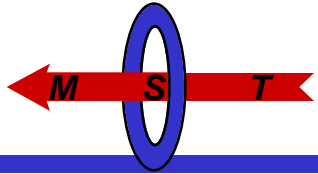
# Power balance for Deuterons

Experimental constraints:

- $\frac{\partial T_D}{\partial t} - \frac{\partial T_{imp}}{\partial t} = 0$
- $T_D = T_{imp} = T_e$
- $P_{CX}$  known (from pyrobolometer and XUV diode)

Deuterium power balance equation reduces to:

$$\frac{3}{2} n_D \frac{(T_e - T_D)}{\tau_{eq}^{D,e}} dV + P_{anom} = P_{CX} + P_{othe}$$



# Equilibration times in PPCD

In PPCD, take  $n_e(0) = 1.6 \times 10^{19} \text{ m}^{-3}$ ,  $T_e(0) = 850 \text{ eV}$ . Then:

$$\tau_{eq}^{D,e} = 50 \text{ ms}, \quad \tau_{eq}^{e,D} = \frac{n_e}{n_D} \tau_{eq}^{D,e} \approx \frac{5}{3} \tau_{eq}^{e,D} \sim 80 \text{ ms}$$

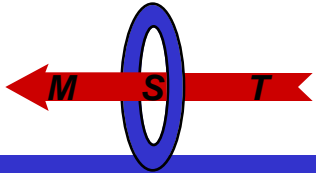
In the plasma core it is calculated that  $Z_{\text{eff}} \sim 5$ , due to an unknown mix of impurities, that is likely dominated by helium-like aluminum. Supposing the impurities are all helium-like Al gives:

$$n_{\text{Al}}/n_e \sim 1/39, \quad n_{\text{Al}}/n_D \sim 2/33, \quad n_D/n_e \sim 3/5$$

Take  $T_D(0) \sim T_{\text{imp}}(0) \sim 300 \text{ eV}$ ,  $\left. \frac{n_{\text{Al}}}{n_e} \right|_{v/a=0} = \frac{1}{39}$  :

$$\tau_{eq}^{D,\text{Al}} = 1.2 \text{ m}$$

$\tau_{eq}^{D,\text{imp}} < \tau_{eq}^{D,\text{Al}}$  for other impurity species present in small amounts.



# Power Balance for Electrons

$$\frac{3}{2} n_e \frac{\partial T_e}{\partial t} = \frac{3}{2} n_e \left( \frac{T_D - T_e}{\tau_{eq}^{e,D}} + \frac{T_{Al} - T_e}{\tau_{eq}^{e,Al}} \right) - P_{oth e}$$

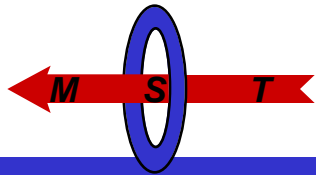
Since  $\frac{\tau_{eq}^{e,Al}}{\tau_{eq}^{e,D}} = \frac{m_{Al}}{m_D} \frac{n_D}{n_{Al}} \frac{Z_D^2}{Z_{Al}^2} \sim \frac{7}{4}$  and  $\tau_{eq}^{D,imp} \leq \tau_{eq}^{D,Al} \ll \tau_{eq}^{e,D}$ ,

we expect  $T_{imp} \sim T_D$  (consistent with observation) and may assume  $T_{Al} \sim T_D$ . The presence of aluminum may then be accounted for by:

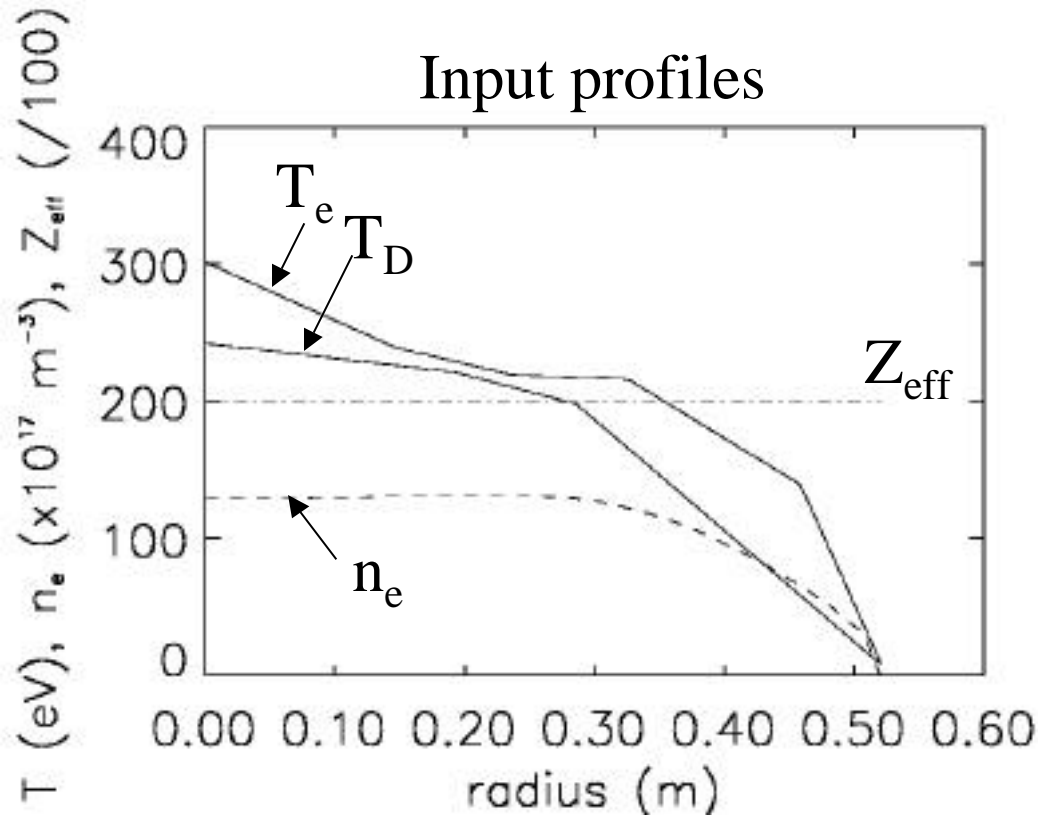
$$\tau_{eq}^{e,D} \rightarrow \frac{7}{11} \tau_{eq}^{e,D} \quad (\text{aluminum enhances energy loss from e})$$

$$\tau_{eq}^{D,e} \rightarrow \frac{7}{11} \frac{33}{31} \tau_{eq}^{D,e} \quad (\text{aluminum enhances energy gain by D})$$

This is true for times longer than  $\tau_{eq}^{D,Al} \sim 1.2$  ms.

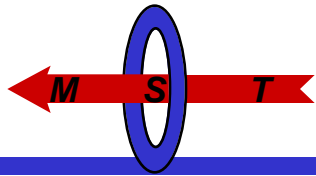


# Global power balance in standard discharges

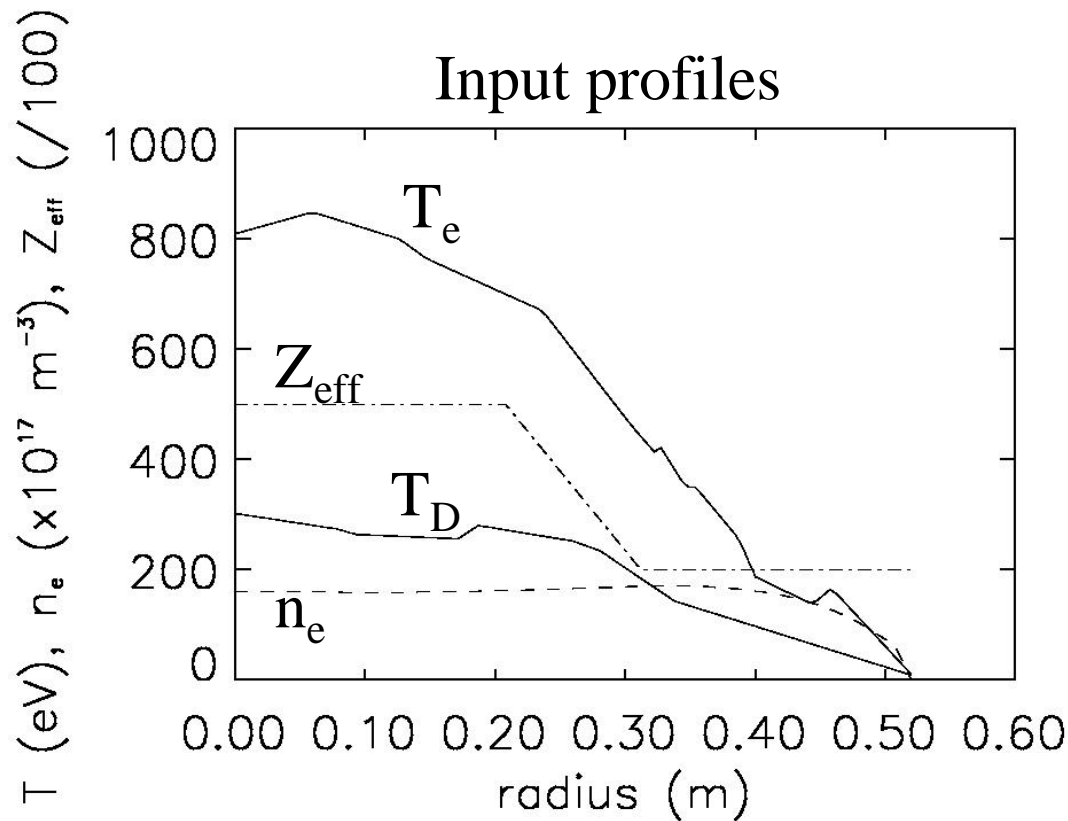


$T_D$  from Rutherford  
 $T_e$  from Thomson  
 $n_e$  from FIR interferometer  
 $Z = 4$  impurities assumed  
flat  $Z_{\text{eff}} = 2$  consistent with earlier  
power balance calculation in low  
current (200 kA) discharges

Volume-integrated classical heating of ions: 80 kW

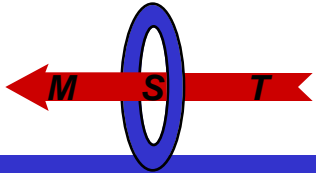


# Global power balance in PPCD discharges



$T_D$  from Rutherford  
 $T_e$  from Thomson  
 $n_e$  from FIR interferometer  
 $Z = 11$  impurities assumed  
 $Z_{\text{eff}}$  profile recently computed  
from bremsstrahlung  
measurement (Anderson, 2001)

Volume-integrated classical heating of ions: 410 kW



# Results of power balance calculation

---

Burst-free PPCD:

Volume-integrated classical heating of deuterons: 410 kW

Ensemble-averaged charge-exchange losses: 460 kW

Net deficit: 50 kW

This would produce:

$$\left\langle \frac{\partial T_D}{\partial t} \right\rangle \sim 3 \text{ eV/ms}$$

Standard plasmas:

Volume-integrated classical heating of deuterons: 80 kW

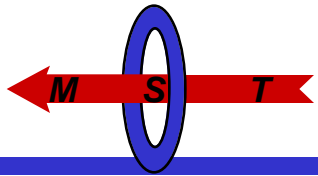
Ensemble-averaged CX losses (between sawteeth): 1.1 MW

Net deficit: ~1 MW

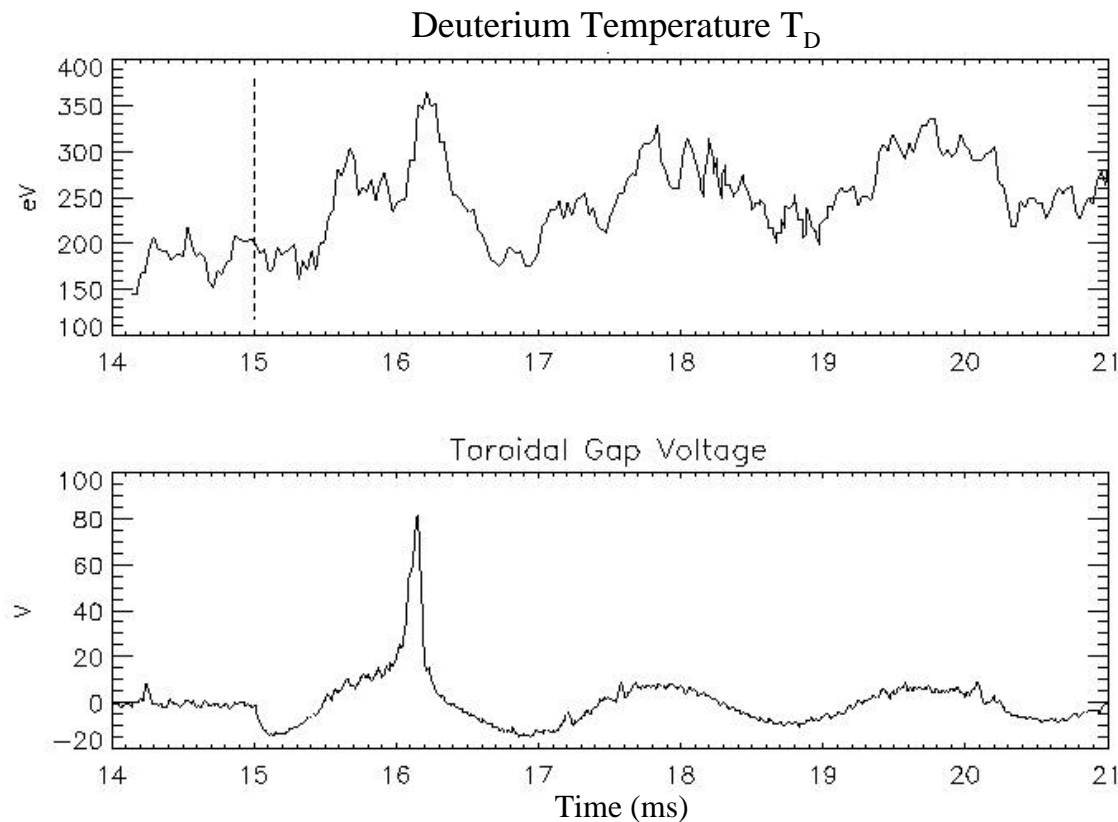
This would produce:

$$\left\langle \frac{\partial T_D}{\partial t} \right\rangle \sim 50 \text{ eV/ms}$$





# Effect of OPCD on Ion Temperature

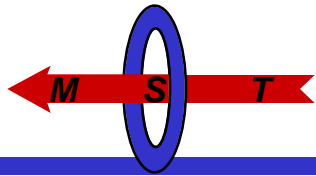


Ensemble parameters:

- 153 discharges
- $I_p=380$  kA
- $n_e=10^{13}$  cm<sup>-3</sup>

$T_D$  measured at  $r/a=0.3$   
OPCD frequency 500 Hz

Figure courtesy Art Blair

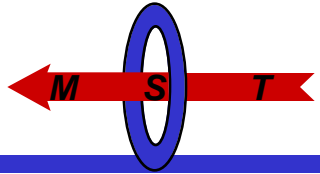


# Conclusions

---

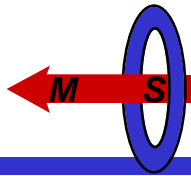
In burst-free PPCD, the observed CX flux slightly exceeds the calculated classical heating rate of deuterons. In the absence of other heating or loss mechanisms, this would result in a decrease in deuteron temperature of about 3 eV/ms, which cannot be ruled out using Rutherford data. Thus the necessity for non-classical ion heating during burst-free PPCD has not been proved.

In standard discharges, the observed CX flux greatly exceeds the calculated heating rate of deuterons, such that the deuterons would cool at a rate of at least 50 eV/ms, were there no other heat source. This temperature decrease can be ruled out using Rutherford data, so the deuterons must be heated non-classically.



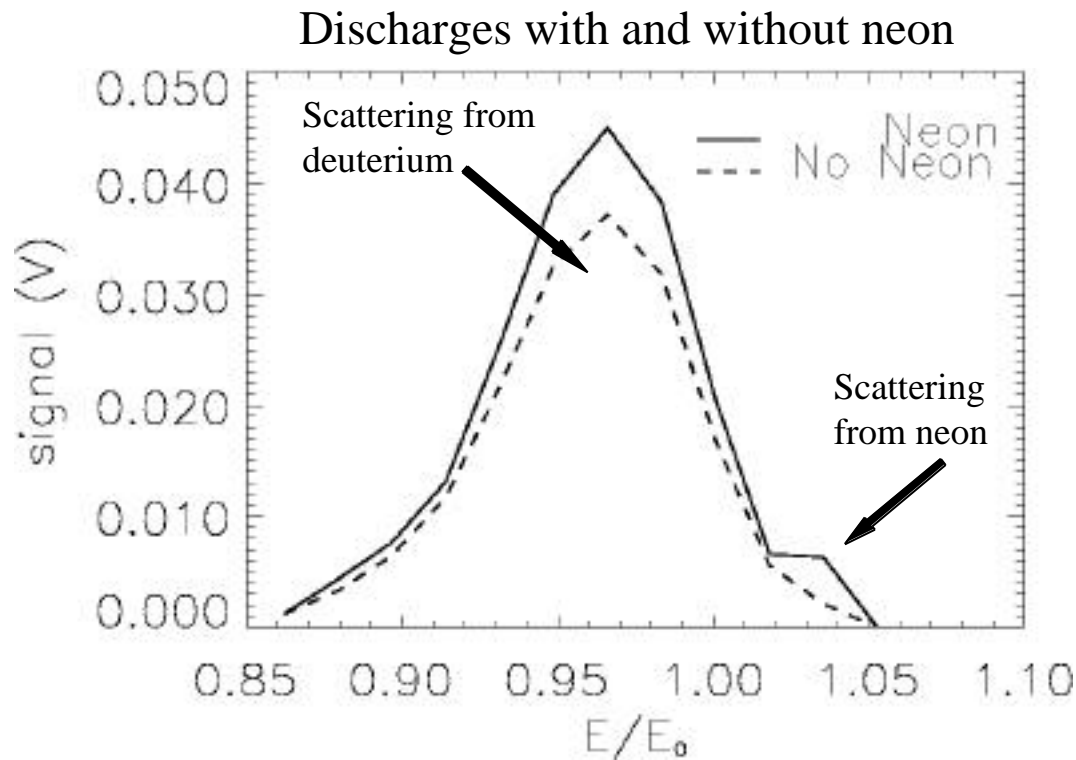
Sign up for reprints!

---

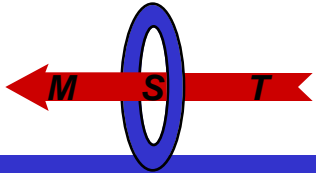


# Effect of neon puff on deuterium density

Deuterium density is 20 % larger in discharges with neon puff than in discharges without neon puff



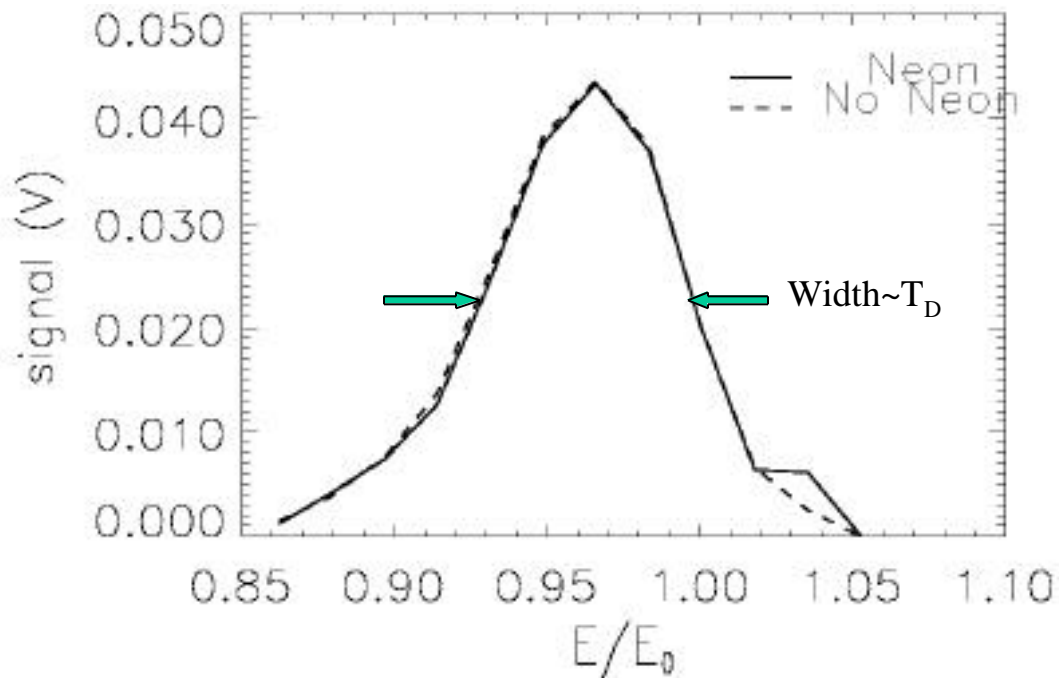
Deuterium density (at  $r = 25 \pm 8$  cm) is proportional to area under deuterium scattering peak (centered at  $E/E_0 \sim 0.97$ ), which is 20 % larger in discharges with neon puff than discharges without neon puff.



# Rutherford Scattering on MST

We have been using Rutherford scattering to measure deuterium temperature, and we hope to use it to estimate  $Z_{\text{eff}}$ .

Discharges with and without neon



Rutherford scattering on MST uses a diagnostic neutral beam of energy  $E_0$  ( $E_0 \sim 17$  KeV). Plot at left shows energy spectrum of beam atoms which have scattered from plasma ions at  $r = 25 \pm 8$  cm (amplitudes have been normalized to have equal area under the curve).

Deuterium temperature  $T_D$  calculated from width of peak.  $T_D$  does not change when neon is puffed.

Perhaps we can estimate  $Z_{\text{EFF}}$  from excess signal at energy  $E/E_0=1.04$  due to scattering from neon.